



Bone mechano-response is driven by locomotion transitions during vertebrate evolution



Saeka Shimochi ¹, Clara Brunet ¹, Margalida Fontcuberta-Rigo ¹, Katja Hrovat¹, Pere Puigbò ^{2,3,7} & Miho Nakamura ^{1,4,5,6,7}

The skeleton supports the muscles in keeping the body upright against gravity while enduring thousands of daily loads. In this study, we investigated non-collagenous bone matrix proteins using osteoblast cell cultures and phylogenetic analyses to identify the molecular mechanisms involved in mechanical loading. The results indicate that several non-collagenous proteins may significantly regulate the bone's response to mechanical stress. Furthermore, we hypothesize that the bone mechano-response is an evolutionary-driven process. The selection analysis indicates that two of the major evolutionary transitions in vertebrate locomotion shaped the roles of non-collagenous proteins in the bone matrix: the water-to-land transition, which increased mechanical stress on the limbs, and the evolution to bipedalism in humans, which altered the distribution of stress on the lower and upper limbs. Fetuin A, positively selected in both evolutionary transitions, showed the most significant expression change during the mechanical stimulation experiments.

The skeleton's main mechanical function is to provide support for muscles to keep the body upright against gravity¹. Furthermore, many bones are subjected to thousands of repetitive loads (impacts) each day¹. Mechanical loading is essential for bone health and development because it plays a critical role in maintaining bone structure, density, and strength². Alterations in the skeleton's dynamic process of bone resorption and formation¹ lead to bone diseases, including osteoporosis, the most common bone problem in elderly populations. A reduction in mechanical loading due to prolonged bed rest³ or long-term exposure to microgravity⁴ can lead to a reduction in bone mass. This understanding supports the general recommendation of weight-bearing exercise (together with getting adequate calcium, sunlight, and vitamin D⁵) to decrease osteoporosis risk⁶. However, the molecular mechanism through which weight-bearing exercises prevent osteoporosis is not fully understood. Several studies in the field of mechanobiology have determined the roles of some cell types, cellular membrane receptors, and bone extracellular matrix (ECM) proteins in mechanical loading^{1,7-9}. Osteocytes function as mechanosensing cells in bone tissue by transduction of mechanical signals to biochemical responses⁷. PIEZO1, as a mechanosensing protein¹⁰, regulates homeostasis via crosstalk of osteoblasts and osteoclasts⁸. Osteopontin is a non-collagenous protein in the ECM related to mechanical stress⁹. However, the bone ECM proteome

comprises hundreds of proteins¹¹ that are poorly understood and may play a major regulatory role in bone responses to mechanical loading (Table S1).

Wolff's law postulates that bone adapts its structure in response to mechanical loading, suggesting that mechanical stimuli can be converted into biological signals that drive bone remodeling¹². Piezoelectricity in bone collagen fibrils, which represent 90% of the organic components of the bone ECM, has been proposed as the mechanism for the conversion of mechanical stimuli into biological signals during weight-bearing exercises¹³. In a previous study, we showed that the electricity mechanically produced in collagen fibrils is stored in the inorganic components of the ECM¹⁴, suggesting that bone ECM plays a critical regulatory role in bone responses to mechanical loading. Since bone ECM plays both a structural role as a mechanical support and a regulatory role as a key component of stem cell niches, we hypothesize that non-collagenous organic components of the bone matrix should have a key function in bone remodeling through mechanical loading. Thus, to identify the key bone ECM proteins, we utilized the principles of biological evolution. We hypothesized that two of the major locomotion transitions in the evolution of vertebrates shaped the role of non-collagenous proteins in humans. The first locomotion transition was the water-to-land transition, which occurred at the time of origin of the tetrapods (~400 Ma), and involved stronger mechanical stress on the limbs

¹Medicity Research Laboratory, Faculty of Medicine, University of Turku, Turku, Finland. ²Department of Biology, University of Turku, Turku, Finland. ³Department of Animal and Food Science, Faculty of Veterinary Medicine, Autonomous University of Barcelona, Bellaterra, Catalonia, Spain. ⁴Laboratory for Biomaterials and Bioengineering, Institute of Science Tokyo, Chiyoda, Tokyo, Japan. ⁵La Salle Campus Barcelona Ramon Llull University, Barcelona, Spain. ⁶Institute of Dentistry, University of Turku, Turku, Finland. ⁷These authors contributed equally: Pere Puigbò, Miho Nakamura. e-mail: pere.puigbo@uab.cat; miho.nakamura@utu.fi

of tetrapods, in addition to ecological, cognitive, and physiological adaptations¹⁵. The second locomotion transition occurred during the evolution to bipedalism in the Hominini (~11.6–4.4 Mya^{16,17}) and was characterized by a striking skeletal adaptation for walking upright on two feet^{17,18}, leading to a differential mechanical stress on arms (less stress) and legs (more stress). Furthermore, other locomotion transitions in the evolution of vertebrates¹⁹ may have played a role in shaping the structure and composition of the bone ECM proteins.

Results

Conservation of bone ECM proteins

Humans (*Homo sapiens*) are vertebrates that have acquired the spinal function to support the body against gravity and achieve upright bipedal locomotion²⁰. Here, we hypothesize that poorly conserved bone ECM proteins, with a large number of adaptive mutations during major locomotion transitions in the evolution of vertebrates, play a major role in bone mechano-responses to mechanical loading in humans. Zebrafish (*Danio rerio*) and humans share more than 98% of bone ECM protein families based on data from the Phylobone database¹¹. These proteins show a wide range of amino acid conservation (percentage of identity in pairwise

sequence alignments from 0.00% to 99.86%) (Fig. 1a, Table S2). Highly conserved homologous proteins between zebrafish and human are also structurally conserved (Table S3). Furthermore, some homologous proteins with poorly conserved amino acid sequences are structurally conserved due to functional constraints of the protein (e.g., Fetuin A, also known as Alpha-2-HS-glycoprotein) (Fig. 1a, b, Table S4).

To test the conservation hypothesis of bone ECM protein mechano-responses, we cultured osteoblast cells under static and mechanical stimulation conditions and quantified protein expression levels of ten selected bone ECM proteins based on an initial screening of the conservation level between human and zebrafish proteins (Fig. 1). The selected proteins for the mechanical stimulation experiments included those with low, medium, and high similarity in their amino acid sequences (Fig. 1a). Seven proteins (osteonectin, alkaline phosphatase [ALP], transforming growth factor-β3 [TGF-β3], osteopontin, bone sialoprotein [BSP], annexin A1, and R-spondin 1 (RSPO1) have similar sequence and structure conservation values. However, three poorly conserved proteins at the sequence level (MATN3, fetuin A, and fetuin B) are moderately conserved at the structure level (Fig. 1a, b, Table S4). Moreover, we performed a selection analysis (see Materials and Methods) of all protein groups ($N = 255$) from the Phylobone

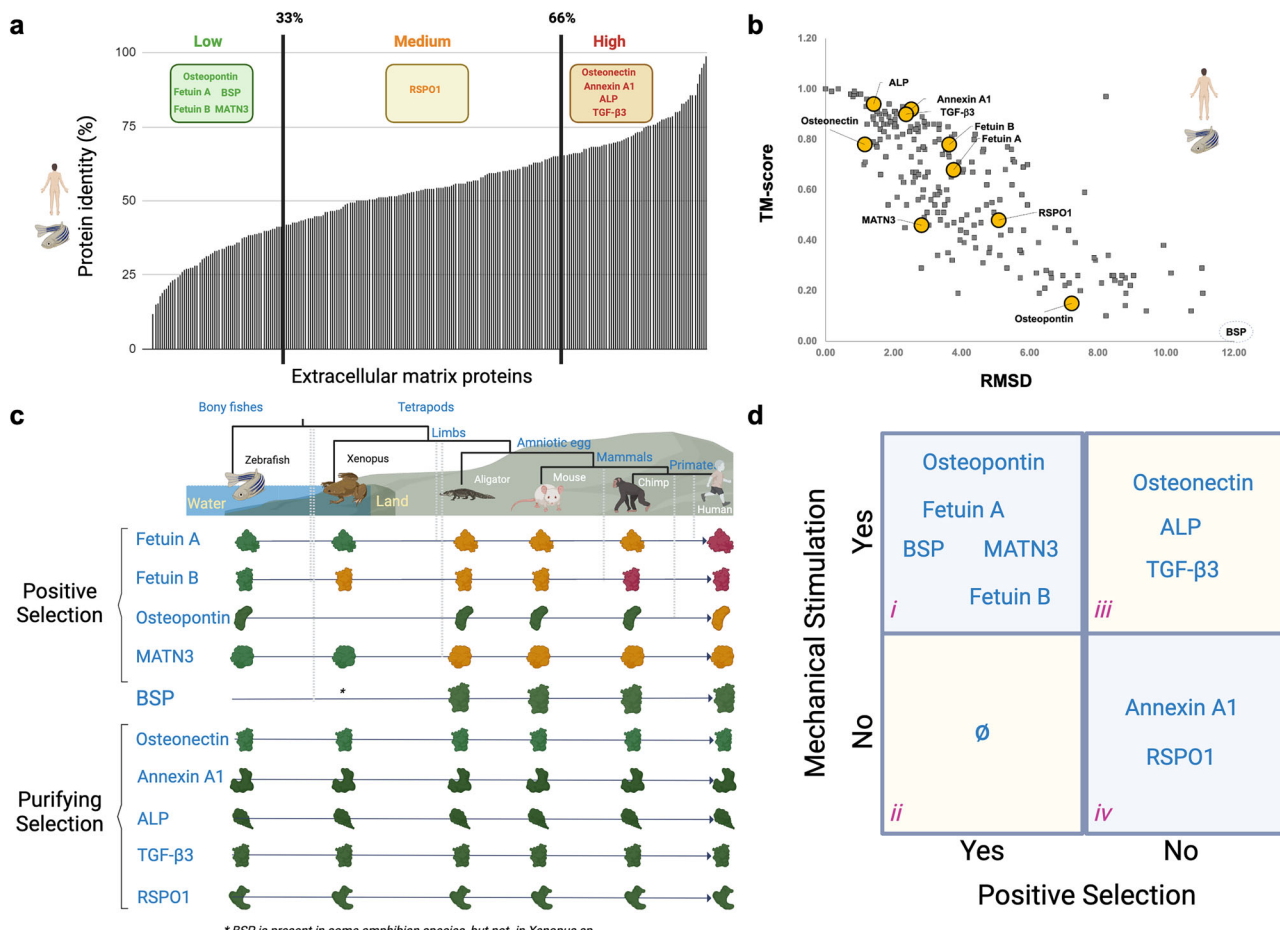


Fig. 1 | Analysis of the evolution of bone ECM proteins in vertebrates.

a Percentage identity of bone ECM homologous proteins between *H. sapiens* and *D. rerio* (Table S2). b Correlation of the root mean square deviation (RMSD) and the template modeling score (TM-Score) of bone ECM homologous proteins between *Homo sapiens* and *Danio rerio* (full results are available in supplementary Table S3). c Schematic representation of the positive selection analysis of bone ECM proteins in vertebrate evolution (full results are available in Tables S4–6). d Contingency table of mechanical stimulation and positive selection. The table is divided into four groups. Proteins in group i (osteopontin, fetuin A, fetuin B, BSP, and MATN3) showed expression differences under mechanical stimulation and experienced positive

selection during vertebrate evolution. Group ii proteins exhibited no positive selection and no differential expression under mechanical stimulation. None of the proteins tested belonged to group ii. The proteins in group iii (osteonectin, ALP, and TGF-β3) were under purifying selection and exhibited differences in protein expression under the static versus the mechanical stimulation conditions. The proteins in group iv (annexin A1 and RSPO1) were under purifying selection and exhibited no differences in protein expression during the mechanical stimulation experiments. Created in BioRender. Nakamura, M. (2025) <https://BioRender.com/0lkt0g1>.

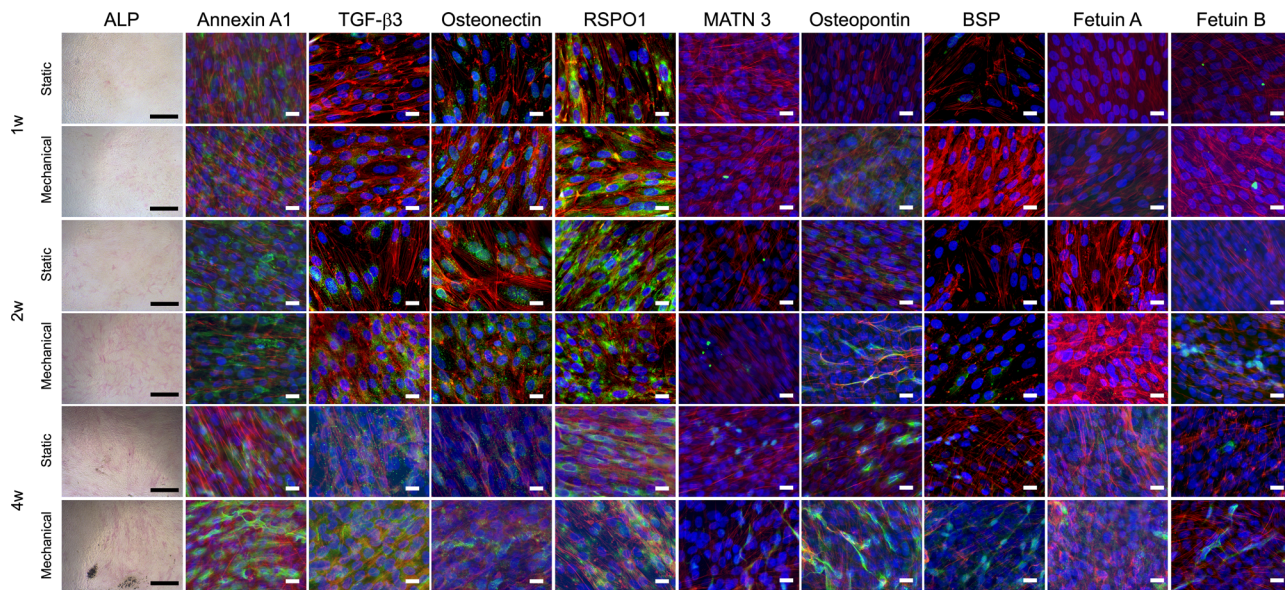


Fig. 2 | Staining of osteoblasts with or without mechanical stimulation. Osteoblasts were cultured in osteoinductive media with or without mechanical stimulation. The cells under the static condition started the osteoblast differentiation after 1 week and differentiated into mature osteoblasts after 4 weeks. The cells exposed to mechanical stimulation differentiated into osteoblasts after 2 weeks, and mineral deposition occurred after 4 weeks. ALP staining revealed that the mechanical stimulation enhanced osteoblast differentiation. Scale bar for ALP images = 500 μ m. Immunofluorescent staining shows that the osteoblasts expressed the target proteins. Merged images of actin (rhodamine phalloidin, red), nuclei (Hoechst, blue) and the targeted proteins (green) are shown. The red, green, and blue color-

separated images are available in Fig. S1–5. Four proteins (RSPO1, annexin A1, osteonectin, and TGF- β 3) were expressed from early to late stages of osteoblast differentiation. Two proteins (RSPO1 and annexin A1) were expressed under both the static and mechanical stimulation conditions. Five proteins (BSP, MATN3, osteopontin, fetuin A, and fetuin B) were observed as dot-like structures in the early stage of osteoblast differentiation and bundle-like structures or aggregated structures in the late stage of osteoblast differentiation. Scale bar for immunofluorescent images = 100 μ m.

database¹¹ to determine the putative effect of evolutionary transitions in mechano-skeletal adaptations to mechanical loading.

Mechanical loading experiments

We speculated that highly conserved bone ECM proteins (under purifying selection) play a major role in bone homeostasis of vertebrates. In contrast, poorly conserved proteins (under positive selection in the major locomotion transitions of evolution (Fig. 1c)) are crucial to achieve mecano-skeletal adaptations in the evolution of vertebrates, including upright bipedal locomotion in humans. Indeed, the expressions of poorly (osteopontin, BSP, fetuin A, and fetuin B) and moderately (MATN3) conserved proteins (Fig. 1d) was enhanced in osteoblasts under mechanical stimulation conditions (Figs. 2 and 3). The osteoblast-like cells were confluent after 1 week, and osteoblast differentiation was observed in some cells, as indicated by ALP staining (Fig. 2). The ALP-positive area increased with culture time. Under the static condition, osteoblast differentiation started after 1 week and differentiated into mature osteoblasts after 4 weeks. The cells exposed to mechanical stimulation differentiated into osteoblasts after 2 weeks, and mineral deposition occurred after 4 weeks. ALP staining revealed that the mechanical stimulation enhanced osteoblast differentiation.

Immunofluorescent staining showed that the osteoblasts expressed the target proteins, including annexin A1, TGF- β 3, osteonectin, RSPO1, MATN3, osteopontin, BSP, fetuin A, and fetuin B (Fig. 2). Three proteins (RSPO1, annexin A1 and osteonectin) were expressed from early to late stages of osteoblast differentiation. Two proteins (RSPO1 and annexin A1) were expressed under both static and mechanical stimulation conditions. TGF- β 3 expression was weak after 1 week but gradually increased after 2 weeks. Two proteins (BSP and MATN3) were seen as dot-like structures after mechanical stimulation for 2 weeks and as bundle-like structures after mechanical stimulation for 4 weeks. The expression of osteopontin was weak after 1 week under the mechanical stimulation condition and after 2 weeks under the static condition. After 4 weeks, osteopontin was seen as dot-like structures under the static condition and as bundle-like structures under the

mechanical stimulation condition. The expression of fetuin A was weak after 2 weeks and increased after 4 weeks. After 4 weeks, fetuin A was seen as dot-like structures under the static condition and as aggregated structures under the mechanical stimulation condition. The expression of fetuin B was weak after 1 week of mechanical stimulation, but increased after 2 weeks under the mechanical stimulation condition. After 2 weeks and 4 weeks of mechanical stimulation, fetuin B was observed as bundle-like structures.

Western blotting revealed that there were no significant differences between the static and mechanical stimulation conditions in the expressions of RSPO1 and annexin A1 (Fig. 3). The expressions of the other target proteins, including TGF- β 3, osteonectin, MATN3, osteopontin, BSP, fetuin A, and fetuin B was increased ~1.5–2-times under the mechanical stimulation condition compared to the static condition. After mechanical stimulation for 2 weeks, fetuin A expression was 6 times greater than in the static condition. Osteonectin and BSP expression increased between 2 and 4 weeks under the mechanical stimulation condition but not under the static condition.

Evolutionary adaptations

Positive selection, also known as Darwinian selection, is an evolutionary process in which advantageous mutations thrive in the population and promote the emergence of new phenotypes²¹. The proteins under positive selection during the studied locomotor transitions in vertebrate evolution (osteopontin, BSP, fetuin A, fetuin B, and MATN3) (Fig. 1c, Tables S5 and S6) exhibited increased expression during mechanical stimulation (Fig. 1d). These proteins showed a positive ratio of non-synonymous and synonymous mutations ($dN/dS > 1$). Notably, we could not find any protein under positive selection with no differential expression under the mechanical stimulation condition (Fig. 1d). These results are in agreement with the conservation hypothesis, i.e., proteins with a large number of accumulated adaptive mutations (positive selection) during locomotion transitions play a major role in bone mecano-responses to mechanical stimulation (Fig. 4).

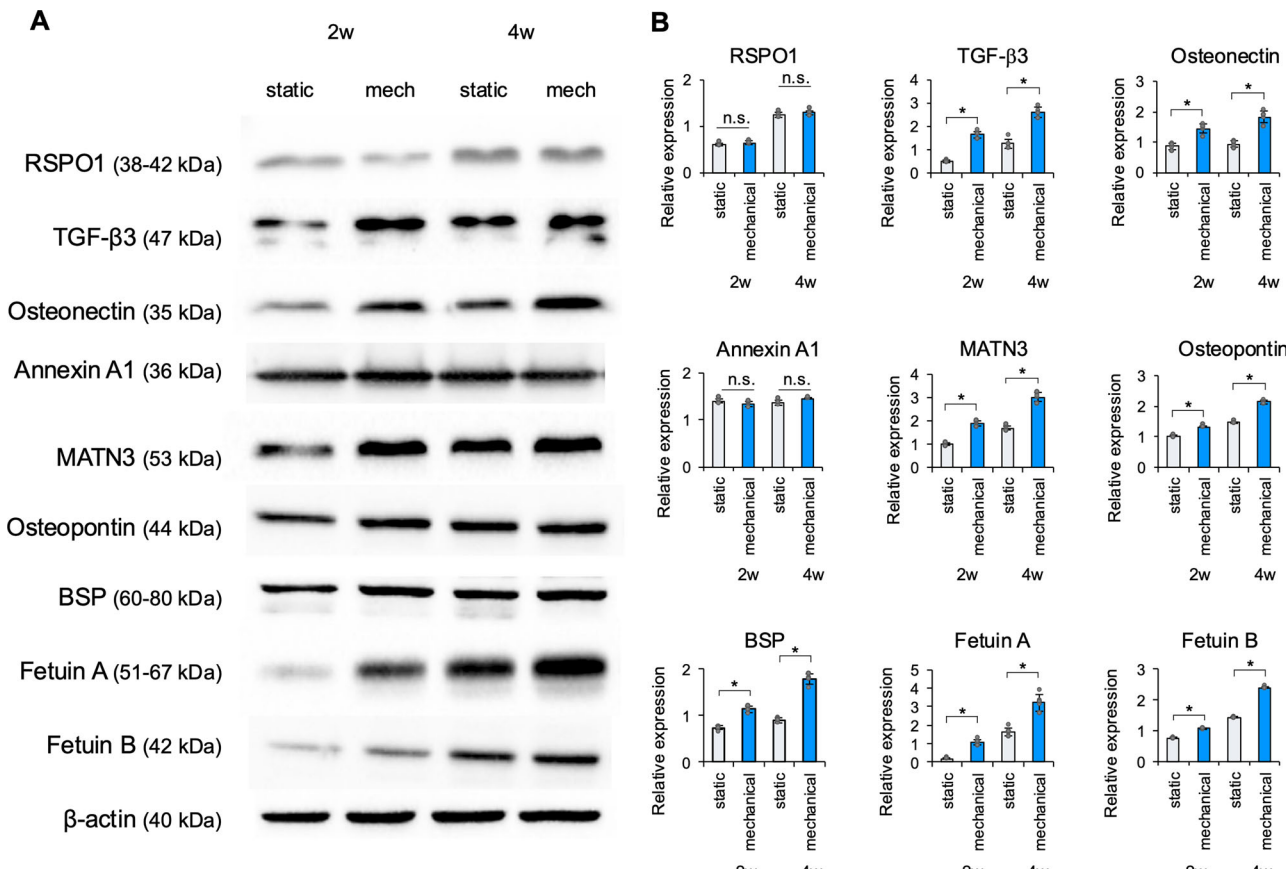


Fig. 3 | Western blot analyses of osteoblasts with or without mechanical stimulation. A Western blot of the cell lysates of the osteoblasts cultured in osteoinductive media with or without mechanical stimulation for 2 and 4 weeks. B Densities of western blotting bands of the target proteins normalized with β -actin. There were no significant differences in the expressions of RSPO1 and annexin A1 between the static and mechanical stimulation conditions. The expressions of the other target proteins (TGF- β 3, osteonectin, MATN3, osteopontin, BSP, fetuin A, and fetuin B) was \sim 1.5–2-times greater under the mechanical stimulation condition compared to

the static condition. As compared with the static condition, the expression of fetuin A was six times greater with mechanical stimulation for 2 weeks. Osteonectin and BSP expression increased between 2 and 4 weeks under the mechanical stimulation condition but not under the static condition. Data are reported as means \pm standard deviation (SD). * p $<$ 0.05 for the comparison of the static condition versus the mechanical stimulation condition. n = 5 for each experiment. n.s. not significant p $>$ 0.05.

The opposite of positive selection is purifying selection, also known as negative selection, a process whereby adverse mutations are eliminated from the population²². Conserved bone ECM proteins throughout vertebrate evolution, under purifying selection, are expected to play a major role across vertebrates (from zebrafish to human), independently of mechanical stimulation and static conditions. The expression patterns of two proteins under purifying selection (RSPO1 and annexin A), were not significantly altered by the mechanical stimulation experiments (Fig. 1d). However, three proteins (osteonectin, ALP, TGF- β 3), with dN/dS < 1 between zebrafish and human (under purifying selection), showed enhanced expression during the mechanical stimulation experiments (Fig. 1c, d, Tables S5 and S6).

Discussion

Our results present evidence of selection associated with locomotion-related loading regimes in the bone ECM proteome, raising the question of how these changes have accumulated. However, this study focuses on a limited set of model species and two major locomotor transitions. Given the small taxon sample and the complexity of vertebrate evolution, it is not possible to determine specific evolutionary models. Furthermore, other significant transitions—such as those from early tetrapods to amniotes, or from non-mammalian synapsids to mammals—may also involve important adaptive changes¹⁹. As such, our findings should be seen as addressing a subset of the broader evolutionary landscape, with further research needed to explore additional transitions.

The proteins under positive selection showed higher expression rates during the mechanical stimulation experiments compared to the static condition, making positive selection an evolutionary marker of their key role. We identified these associations in all proteins under positive selection (five out of ten proteins: Osteopontin, Fetuin A, BSP, MATN3, and Fetuin B), each showing significant differences in expression during mechanical stimulation experiments, in line with the conservation hypothesis. We hypothesize that these proteins experienced adaptive mutations during locomotion transitions in vertebrate evolution. In contrast, proteins not under positive selection showed variable responses: three out of five exhibited differential expression, whereas two did not—likely reflecting additional regulatory or functional constraints beyond those encompassed by the conservation hypothesis.

Differential protein expression rates in proteins under both positive and purifying selection arise due to genetic, genomic, epigenetic, and post-translational modification factors. Gene duplications have contributed to the evolution of the vertebrate skeleton. For example, after vertebrates evolved the mineralized skeleton, the proteins from the secretory calcium-binding phosphoprotein (such as proteins SPARC [i.e., osteonectin] and SPARCL1) originated by whole genome duplication²³. Gene duplications can lead to novel functions, as well as to a beneficial increase in gene expression²⁴. However, no significant differences were found between human and zebrafish in the gene copy number of the selected proteins (Table S7). Differential expression rates

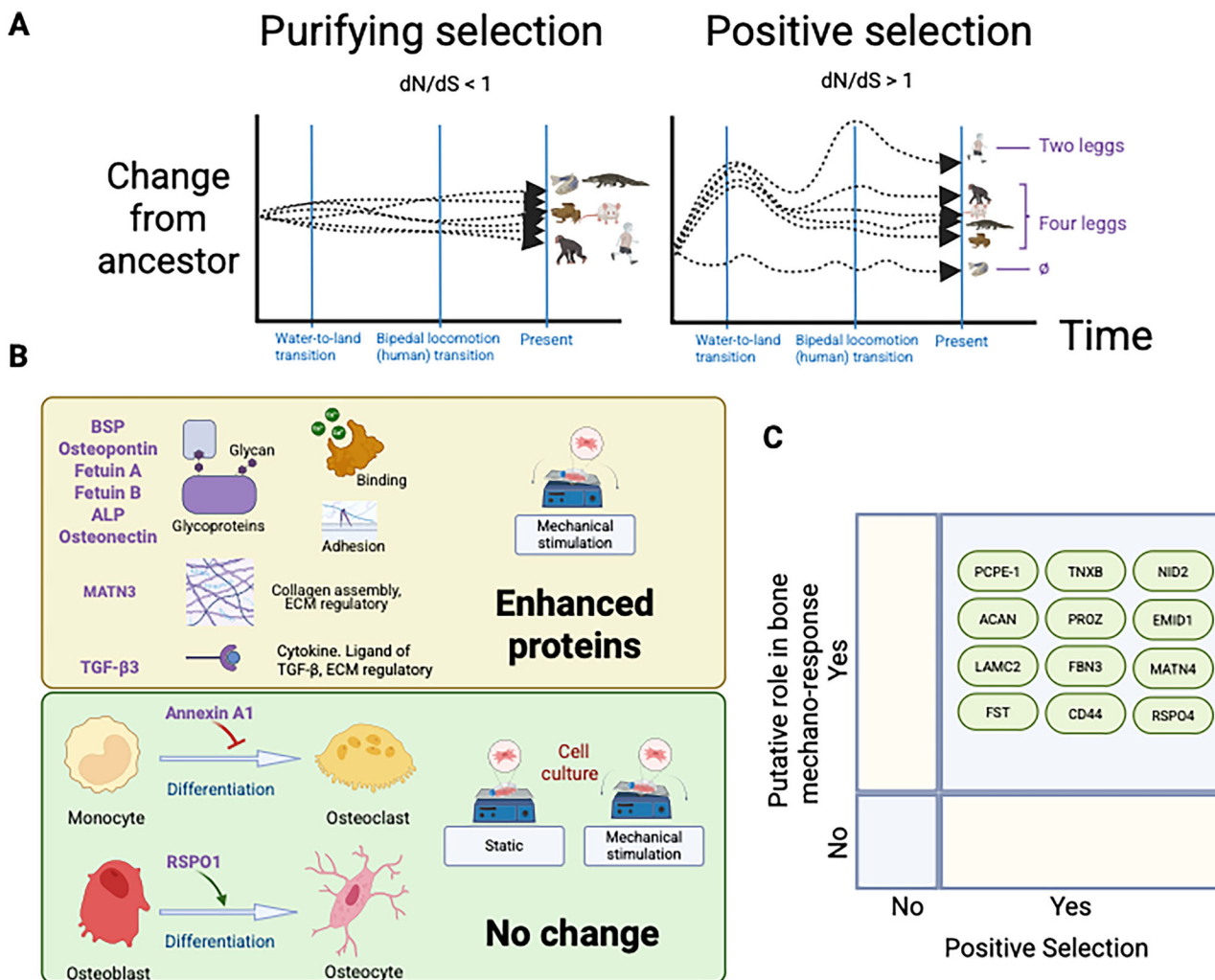


Fig. 4 | Proteins involved in bone mechano-responses. A Schematic representation of proteins under purifying ($dN/dS < 1$) and positive ($dN/dS > 1$) selection during the water-to-land transition in terrestrial vertebrates and the bipedal locomotion transition in humans. Proteins in the bone extracellular matrix (ECM) involved in mechano-response are hypothesized to accumulate adaptive mutations (shown as positive selection) during the evolutionary transitions that altered locomotion mechanisms in vertebrates. B In the mechanical stimulation experiments, the expression of eight regulatory bone ECM proteins was enhanced: six glycoproteins (BSP, osteopontin, fetuin A, fetuin B, and osteonectin) with functions involved in

molecular binding (e.g., binding of calcium) and cell adhesion and two non-glycoproteins (MATN3 involved in collagen assembly, and the cytokine, TGF- β 3). C Additional bone ECM proteins, that present signs of positive selections during water-to-land and bipedalism transitions, and with functions potentially involved in bone mechano-responses (TNXB Tenascin-X, ACAN Aggrecan core protein, NID2 Nidogen-2, PROZ Vitamin K-dependent protein Z, EMID1 EMI domain-containing protein1, LAMC2 Laminin subunit gamma-2, FBN3 Fibrillin-3, MATN4 Matrilin-4, FST Follistatin, CD44 CD44 antigen, RSPO4 R-spondin-4). Created in BioRender. Nakamura, M. (2025) <https://BioRender.com/v5u4w7l>.

between the static and mechanical stimulation conditions may also have arisen due to translational selection (i.e., a differential adaptation of the protein to the translational machinery of the cell that results in higher expression rates)²⁵. Translational selection is a strong driver of evolution of vertebrate genomes that shape codon usage patterns²⁶, and it has been well described in the three domains of life (eukaryotes, bacteria and archaea)^{27,28}. Although the selected proteins are putatively highly expressed based on codon usage biases (Table S8), codon biases may not explain functional adaptations, such as cells growing under mechanical and static conditions. Furthermore, non-collagenous proteins in the bone matrix are in a highly complex environment, closely intertwined with collagen fibrils, and are differentially expressed in different anatomical locations and body tissues (Table S9 and S10). Thus, further experiments beyond the scope of this article are needed to determine the role of epigenetics, post-translational modifications and protein-protein interaction factors in the gene expression of bone ECM proteins²⁹.

Mechanical loading increases bone mass by stimulating bone-forming osteoblasts and osteocytes through a cascade of intracellular pathways involving several biomolecules, such as nitric oxide, prostaglandins, bone morphogenetic proteins (BMP), and Wnts³⁰. Moreover, experiments in knockout mice have shown the role of an ECM protein (osteopontin) in response to mechanical stimulation⁹. In this study, we identified eight proteins that exhibited higher expression during mechanical stimulation (ALP, BSP, fetuin A, fetuin B, MATN3, osteonectin, osteopontin, and TGF- β 3) and two proteins with no differential expression in mechanically stimulated cell cultures (annexin A1 and RSPO1). Proteins in the bone ECM can be classified into structural and regulatory roles¹¹. Additionally, regulatory proteins can be further divided into those that regulate bone matrix structure and those that control bone cell growth and differentiation. In our experiments, seven proteins that exhibited a higher expression during mechanical stimulation are involved in the regulation of the bone matrix, with functions that encompass glycoproteins (BSP, osteopontin, osteonectin, ALP, fetuin A, and fetuin B), calcium-binding proteins (BSP), and

collagen assembly regulation (MATN3) (Fig. 4B, Table S11–13). In addition, the expression of the cytokine TGF- β 3, which regulates the early stages of osteoblast differentiation³¹, was enhanced by mechanical stimulation. However, the proteins involved in the regulation of osteoclast differentiation (annexin A1) and osteoblast differentiation to osteocytes (RSPO1) were not enhanced by mechanical stimulation.

The water-to-land transition in vertebrates involved the evolution of the skeletal system to support locomotor activity in the terrestrial environment³². The evolution of the skeletal system has been linked with immune molecules; for example, the receptor activator of the nuclear factor- κ B ligand (RANKL)–RANK system has been conserved since the emergence of the adaptive immune system with T and B cells in cartilaginous fish³². Furthermore, during the evolution to bipedalism in humans, the skeletal system was adapted for walking regularly in an upright position^{17,18}. This involved molecular changes in the BMP³³. In agreement with the conservation hypothesis presented in this study, functionally relevant proteins can be predicted by observing changes during the two significant locomotion transitions in the evolution of vertebrates (Fig. 4A). Fetuin A (and Osteopontin⁹) showed the most striking change in protein expression during mechanical stimulation, with the immunofluorescent staining and Western blotting revealing that its expression was enhanced in osteoblasts by mechanical stimulation (Figs. 2 and 3). In agreement with the conservation hypothesis, fetuin A exhibits strong signs of positive selection during the water-to-land transition of vertebrates and the bipedalism transition in humans. Furthermore, fetuin A protein shows low amino acid conservation (Fig. 1a, Table S2) and medium structural conservation (Fig. 1b, Table S4). Fetuin A is known to influence the production of inflammation mediators, inhibit ectopic calcification in soft tissue³⁴, and reduce biomaterial particle-induced osteolysis³⁵. Therefore, Fetuin A is a strong candidate as a biomarker for skeletal disorders like osteoporosis and rheumatoid arthritis, and a potential target for drug treatment.

The first line of osteoporosis treatments is bisphosphonates and the monoclonal RANKL antibodies. The targets of these drugs are calcium minerals in bone ECM and RANK receptors on osteoclast precursors³⁶, respectively. Among the selected proteins, fetuin A is potentially the strongest candidate for further exploration. However, additional proteins involved in mechanical loading (ALP, BSP, fetuin B, MATN3, osteonectin, osteopontin, and TGF- β 3) could be potential drug targets for the treatment and prevention of osteoporosis. Moreover, other proteins of the bone ECM that play a regulatory role, such as those with roles in osteogenesis and bone degradation³⁷, may be targets for new treatments for bone regeneration¹¹. Furthermore, we speculate that ECM proteins with signs of positive selection during the water-to-land and bipedalism transitions, with regulatory functions in the bone matrix (Fig. 4C), may play a significant role in the bone mechano-response to mechanical loading.

Methods

Protein sequences

Protein sequences were collected from the Phylobone database¹¹. This database contains a list of 255 putative bone ECM proteins found in 31 species of vertebrates, including the species selected for this study. We selected one representative species from each of the major taxonomic groups of vertebrates: bony fishes (*D. rerio*), amphibians (*Xenopus laevis*), reptiles (*Alligator sinensis*), rodents (*Mus musculus*), and primates (*Pan troglodytes* and *H. sapiens*).

Protein sequence similarity (percentage of identity between *D. rerio* and *H. sapiens*)

All protein homologs from *H. sapiens* and *D. rerio* were compared. Sequence pairs were aligned using the program Muscle³⁸, and an in-house script was utilized to calculate the percentage of identity between pairs of proteins (i.e., the number of amino acid matches and mismatches between

H. sapiens and *D. rerio*). In cases where the protein sequences of *D. rerio* were not found (e.g., BSP), we assigned 0.0% identity for operational reasons.

Selection of proteins for mechanical stimulation experiments

Ten bone ECM proteins were selected for the mechanical stimulation experiments (Table S11 and Fig. 1a) based on the following: 1) the length of the sequences (proteins between 250 and 1000 amino acids long); 2) percentage of identity (low: <33.0%, medium: ≥33.0–66.0%, and high: ≥66.0%); and 3) putative functional importance of these proteins in bone ECM based on the literature¹¹. The ten proteins selected were: 1) five proteins, with less than 30% of protein identity were selected (Osteopontin, Fetuin A, Fetuin B, Bone sialoprotein (BSP), and RSPO1); 2) one moderately conserved protein was selected (Matrilin 3 (MATN3)); and 3) three highly conserved proteins (osteonectin (also known as secreted protein acidic and rich in cysteine, SPARC), annexin A1, ALP, and TGF- β 3).

Pairwise structure alignment

All proteins from *H. sapiens* were compared with their homologs in *D. rerio* (when the sequence was available) using a pairwise structure alignment tool to align the 3D structure of the protein³⁹. Predictions of protein structures were based on artificial intelligence AlphaFold models⁴⁰. The root mean square deviation (RMSD) and the TM-Score were used to quantify similarities between the protein structures⁴¹.

Preparation of sequences for the selection analysis

Multiple sequence alignments (MSAs) were performed, and phylogenetic trees were reconstructed using the server NGPhylogeny⁴². This server aligns proteins (raw MSAs) using the program MAFFT⁴³, and removes non-conserved regions in the alignment (clean MSAs) with the program Block Mapping and Gathering with Entropy (BMGE)⁴⁴. The Clean MSAs are used for the reconstruction of phylogenetic trees using the program PhyML⁴⁵. The raw MSAs together with the corresponding coding sequences of DNA, were used as input for the server PAL2NAL⁴⁶ to convert the raw MSAs of proteins to the corresponding DNA sequence alignment of codon alignment (codon MSAs). The resulting codon MSAs were used for the calculation of non-synonymous (dN) and synonymous (dS) substitution rates.

Codon pairwise alignments

Pairwise alignments of protein sequences were performed with the Sequence Manipulation server⁴⁷. The Smith-Waterman algorithm and the BLOSUM62 matrix were used to perform the pairwise alignments. These protein alignments were converted into codon pairwise alignments using the program PAL2NAL⁴⁶ and used for the calculation of dN and dS ratios.

Selection analysis based on dN and dS ratios

Predictions of positive selection were estimated with the dN/dS ratio, which is the ratio of the number of non-synonymous substitutions per non-synonymous site (pN) to synonymous substitutions per synonymous site (pS)⁴⁸. We have analyzed the dN/dS ratio in five vertebrate species (Table S1) using an indel-aware algorithm (<https://github.com/clarabrunet/iDNDs>) that analyzes the ratio at different levels of the species tree and uses an indel-aware table of expected synonymous and non-synonymous mutations (Table S14). Proteins with a dN/dS > 1 are considered to be under positive selection. To assess the statistical significance of positive selection, a binomial z-test was performed on site-specific dN/dS values (i.e., codon-wise dN/dS values were obtained for each sequence pair). The objective was to determine whether the proportion of codon sites under positive selection (dN/dS > 1) was significantly higher than expected under the null hypothesis of neutral evolution. The one-tailed binomial test was applied using the binomtest function from the SciPy package in Python⁴⁹. The resulting p-value was used to determine statistical significance, with thresholds set at $p \leq 0.05$ (*), $p \leq 0.01$ (**), and $p \leq 0.001$ (***)⁵⁰, corresponding to confidence levels of 95%, 99%, and 99.9%, respectively.

Cell culture

Osteoblast-like cells (MG-63 cell line) were seeded into 12-well cell culture plates at a density of 2×10^4 cells/well and cultured in Dulbecco's modified Eagle's medium (DMEM; Gibco 21969-035, NY, USA) supplemented with 10% fetal bovine serum (Gibco 10270-098, NY, USA), L-glutamine (Gibco 25030081, NY, USA), and 100 U/ml penicillin-streptomycin (Gibco 15140-122, NY, USA) in a humidified atmosphere of 5% CO₂ in air at 37 °C. After reaching confluence, the cells were cultured in osteoinductive medium including 100 nM dexamethasone (Sigma-Aldrich, St. Louis, MO, USA), 10 mM β-glycerophosphate (Sigma-Aldrich, St. Louis, MO, USA) and 50 µg/ml ascorbic acid (Sigma-Aldrich, St. Louis, MO, USA). The cell culture plates were placed on a see-saw rocker for 30 min/day to induce mechanical stimulation⁵⁰.

After culturing for 1, 2, and 4 weeks, the cells were fixed in 4% paraformaldehyde for 20 min. To visualize the differentiation into osteoblasts, the cells were stained with ALP (Sigma-Aldrich, St. Louis, MO, USA) and observed using a microscope (Olympus BX60).

Immunofluorescent staining

After the cell culture for 1, 2 and 4 weeks, the cells were fixed with 4% paraformaldehyde for 20 min. The cells were incubated in a solution for blocking and permeabilization, including 0.2% Tween 20 and 1% bovine serum albumin (BSA) in phosphate-buffered saline (PBS). Anti-human primary antibodies (osteonectin, PA578178; RSPO1, PA5121183; TGF-β3, PA599186; annexin A1, 713400; MATN3, PA520727; fetuin A, PA551594; fetuin B, PA529468; BSP, Bs-2668R; osteopontin, 229521AP, Invitrogen, CA, USA) diluted at a 1:100 in PBS including 0.2% BSA were added for 1 h at room temperature. Following PBS washes, the cells were incubated in a secondary antibody (Alexa Fluor™ 488 Goat anti-rabbit IgG antibody, A11008, CA, USA) diluted at a 1:500 in PBS including 0.2% BSA. The cells were stained for rhodamine phalloidin (Invitrogen R415, CA, USA) and Hoechst 33258 (Sigma-Aldrich, 94403, St. Louis, MO, USA). The fluorescent signals were observed using a fluorescence microscope (Olympus BX60).

Western blotting

After the cell culture for 2 and 4 weeks, the cells were lysed with 300 µl of lysis buffer containing 50 mM Tris-HCl (pH6), 150 mM NaCl and 1% Triton X-100. The cells were scraped, collected into tubes and sonicated for 10 seconds. The cell lysates were frozen at -80 °C until use.

The protein samples were mixed with 4× Laemmli sample buffer (Bio-Rad 1610747, CA, USA) and heated at 95 °C for 5 min. The protein samples were electrophoresed at 60 V for 15 min and further 120 V for 120 min on 5% stacking gel with 10% (for BSP, Fetusin A, Fetusin B, and MATN3) or 12% (for osteonectin, RSPO1, TGF-β3, annexin A1, osteopontin, and β-actin) SDS polyacrylamide. The proteins were transferred from SDS gel to Trans-Blot Turbo Midi 0.2 µm nitrocellulose membrane (Bio-Rad, CA, USA) at 15 V for 30 min using a semi-dry transfer system Trans-Blot® Turbo™ (Bio-Rad, CA, USA). The nitrocellulose membrane was incubated in blocking solution including 5% skim milk in TBST (Tris-buffered saline including 0.1% Tween 20) for 60 min at room temperature with shaking. After washing the nitrocellulose membrane in TBST for 10 min at room temperature with shaking three times, the membrane was incubated in blocking solution including primary antibodies at dilutions of 1:1000 (for Fetusin A and osteopontin) or 1:500 (for BSP, Fetusin B, MATN3, osteonectin, RSPO1, TGF-β3, annexin A1, and β-actin) at 4 °C overnight. Each target protein was analyzed using a separate gel and membrane. No stripping and reprobing were performed. After washing with TBST, goat anti-rabbit IgG horseradish peroxidase (HRP)-conjugated secondary antibody (Invitrogen 31460, CA, USA) was diluted at a 1:10000 in blocking solution and added to the membrane at room temperature for 60 min. After washing with TBST, the protein bands were visualized using a chemiluminescence reagent (Thermo Scientific™ 34585, MA, USA), captured with a ChemiDoc (Bio-Rad, CA, USA) and quantified using Image J software (version 1.41, National Institute of Health).

Statistics and reproducibility

Accurate quantifications of the different samples in the cell study were achieved by performing four independent experiments. All the western blot experiments were conducted at least in duplicate, triplicate, or quadruplicate experiments. The protein bands of the western blotting were presented as a representative of several experiments. Statistical analysis across the experimental groups was performed using the analysis of variance with Tukey's post hoc test for multiple comparisons, using the SPSS software package (version 29, Chicago, IL, USA). The statistically significant level was set at $p < 0.05$ for all the tests. All data have been expressed as mean ± standard deviation.

Reporting summary

Further information on research design is available in the Nature Portfolio Reporting Summary linked to this article.

Data availability

The authors confirm that the data supporting the findings of this study are available within the article. All uncropped and unedited blot images are included as Supplementary Figs. S6–11. The source data behind the graphs in the paper can be found in Supplementary Data 1 (Fig. 3B) and Supplementary Data 2 (Supplementary Tables 1–3).

Received: 19 November 2024; Accepted: 18 November 2025;

Published online: 29 November 2025

References

1. Ding, S. et al. Perception and response of skeleton to mechanical stress. *Phys. Life Rev.* **49**, 77–94 (2024).
2. Iolascon, G., Resmini, G. & Tarantino, U. Mechanobiology of bone. *Aging Clin. Exp. Res.* **25**, S3–S7 (2013).
3. Rolvien, T. et al. Long-term immobilization in elderly females causes a specific pattern of cortical bone and osteocyte deterioration different from postmenopausal osteoporosis. *J. Bone Miner. Res.* **35**, 1343–1351 (2020).
4. Baran, R. et al. Microgravity-related changes in bone density and treatment options: a systematic review. *Int. J. Mol. Sci.* **23**, 8650 (2022).
5. Polzonetti, V., Pucciarelli, S., Vincenzetti, S. & Polidori, P. Dietary intake of vitamin d from dairy products reduces the risk of osteoporosis. *Nutrients* **12**, 1743 (2020).
6. Pinheiro, M. B. et al. Evidence on physical activity and osteoporosis prevention for people aged 65+ years: a systematic review to inform the WHO guidelines on physical activity and sedentary behaviour. *Int. J. Behav. Nutr. Phys. Act.* **17**, 150 (2020).
7. Yan, Y., Wang, L., Ge, L. & Pathak, J. L. Osteocyte-mediated translation of mechanical stimuli to cellular signaling and its role in bone and non-bone-related clinical complications. *Curr. Osteoporos. Rep.* **18**, 67–80 (2020).
8. Wang, L. et al. Mechanical sensing protein PIEZO1 regulates bone homeostasis via osteoblast-osteoclast crosstalk. *Nat. Commun.* **11**, 282 (2020).
9. Fujihara, S. et al. Function and regulation of osteopontin in response to mechanical stress. *J. Bone Miner. Res.* **21**, 956–964 (2006).
10. Coste, B. et al. Piezo1 and Piezo2 are essential components of distinct mechanically activated cation channels. *Science* **330**, 55–60 (2010).
11. Fontcuberta-Rigo, M., Nakamura, M. & Puigbò, P. Phylobone: a comprehensive database of bone extracellular matrix proteins in human and model organisms. *Bone Res.* **11**, 44 (2023).
12. Frost, H. M. Wolff's Law and bone's structural adaptations to mechanical usage: an overview for clinicians. *Angle Orthod.* **64**, 175–188 (1994).
13. Halperin, C. et al. Piezoelectric effect in human bones studied in nanometer scale. *Nano Lett.* **4**, 1253–1256 (2004).

14. Nakamura, M., Hiratai, R. & Yamashita, K. Bone mineral as an electrical energy reservoir. *J. Biomed. Mater. Res. A* **100**, 1368–1374 (2012).
15. MacIver, M. A. & Finlay, B. L. The neuroecology of the water-to-land transition and the evolution of the vertebrate brain. *Philos. Trans. R. Soc. Lond. B Biol. Sci.* **377**, 20200523 (2022).
16. Lovejoy, C. O., Suwa, G., Spurlock, L., Asfaw, B. & White, T. D. The pelvis and femur of *Ardipithecus ramidus*: the emergence of upright walking. *Science* **326**, 71e1–76e1 (2009).
17. Böhme, M. et al. A new Miocene ape and locomotion in the ancestor of great apes and humans. *Nature* **575**, 489–493 (2019).
18. Harcourt-Smith, W. H. E. The first hominins and the origins of bipedalism. *Evol. Edu. Outreach* **3**, 333–340 (2010).
19. Gans, C., Gaunt, A. S. & Webb, P. W. Vertebrate locomotion. In *Comprehensive Physiology* (ed. Prakash, Y. S.) 55–213 (Wiley, 2011).
20. Galbusera, F. & Wilke, H. J. Biomechanics of the spine. In *Basic concepts, spinal disorders and treatments* (2018).
21. Vallender, E. J. & Lahn, B. T. Positive selection on the human genome. *Hum. Mol. Genet.* **13 Spec No 2**, R245–R254 (2004).
22. Cai, J. J. & Petrov, D. A. Relaxed purifying selection and possibly high rate of adaptation in primate lineage-specific genes. *Genome Biol. Evol.* **2**, 393–409 (2010).
23. Kawasaki, K., Buchanan, A. V. & Weiss, K. M. Gene duplication and the evolution of vertebrate skeletal mineralization. *Cells Tissues Organs* **186**, 7–24 (2007).
24. Cardoso-Moreira, M. et al. Evidence for the fixation of gene duplications by positive selection in *Drosophila*. *Genome Res.* **26**, 787–798 (2016).
25. Hopstaken, A. J. P., Große Wichtrup, E. & Jongkees, S. A. K. The great codon escape: vacating codons for genetic code expansion and ribosome stalling. *Isr. J. Chem.* **64**, e202400012 (2024).
26. Doherty, A. & McInerney, J. O. Translational selection frequently overcomes genetic drift in shaping synonymous codon usage patterns in vertebrates. *Mol. Biol. Evol.* **30**, 2263–2267 (2013).
27. Puigbò, P., Romeu, A. & Garcia-Vallvé, S. HEG-DB: a database of predicted highly expressed genes in prokaryotic complete genomes under translational selection. *Nucleic Acids Res.* **36**, D524–D527 (2008).
28. Sharp, P. M., Stenico, M., Peden, J. F. & Lloyd, A. T. Codon usage: mutational bias, translational selection, or both?. *Biochem. Soc. Trans.* **21**, 835–841 (1993).
29. Tanakas, S., Aubin, J. E. & van Wijnen, A. J. Epigenetic control of skeletal homeostasis and diseases. *Bone* **144**, 115797 (2021).
30. Klein-Nulend, J., Bakker, A. D., Bacabac, R. G., Vatsa, A. & Weinbaum, S. Mechanosensation and transduction in osteocytes. *Bone* **54**, 182–190 (2013).
31. Shi, Y. & Massagué, J. Mechanisms of TGF-β signaling from cell membrane to the nucleus. *Cell* **113**, 685–700 (2003).
32. Tsukasaki, M. & Takayanagi, H. Osteoimmunology: evolving concepts in bone-immune interactions in health and disease. *Nat. Rev. Immunol.* **19**, 626–642 (2019).
33. Indjeian, V. B. et al. Evolving new skeletal traits by cis-regulatory changes in bone morphogenetic proteins. *Cell* **164**, 45–56 (2016).
34. Kan, C. et al. Fetuin-A is an immunomodulator and a potential therapeutic option in BMP4-dependent heterotopic ossification and associated bone mass loss. *Bone Res.* **10**, 62 (2022).
35. Jablonski, H. et al. A single intraperitoneal injection of bovine fetuin-A attenuates bone resorption in a murine calvarial model of particle-induced osteolysis. *Bone* **105**, 262–268 (2017).
36. Gao, Y., Patil, S. & Jia, J. The development of molecular biology of osteoporosis. *Int. J. Mol. Sci.* **22**, 8182 (2021).
37. Lin, X., Patil, S., Gao, Y.-G. & Qian, A. The bone extracellular matrix in bone formation and regeneration. *Front. Pharmacol.* **11**, 757 (2020).
38. Edgar, R. C. MUSCLE: multiple sequence alignment with high accuracy and high throughput. *Nucleic Acids Res.* **32**, 1792–1797 (2004).
39. Prlic, A. et al. Pre-calculated protein structure alignments at the RCSB PDB website. *Bioinformatics* **26**, 2983–2985 (2010).
40. Jumper, J. et al. Highly accurate protein structure prediction with AlphaFold. *Nature* **596**, 583–589 (2021).
41. Zhang, Y. & Skolnick, J. TM-align: a protein structure alignment algorithm based on the TM-score. *Nucleic Acids Res.* **33**, 2302–2309 (2005).
42. Lemoine, F. et al. NGPhylogeny.fr: new generation phylogenetic services for non-specialists. *Nucleic Acids Res.* **47**, W260–W265 (2019).
43. Katoh, K. & Standley, D. M. MAFFT multiple sequence alignment software version 7: improvements in performance and usability. *Mol. Biol. Evol.* **30**, 772–780 (2013).
44. Criscuolo, A. & Gribaldo, S. BMGE (Block Mapping and Gathering with Entropy): a new software for selection of phylogenetic informative regions from multiple sequence alignments. *BMC Evol. Biol.* **10**, 210 (2010).
45. Guindon, S. et al. New algorithms and methods to estimate maximum-likelihood phylogenies: assessing the performance of PhyML 3.0. *Syst. Biol.* **59**, 307–321 (2010).
46. Suyama, M., Torrents, D. & Bork, P. PAL2NAL: robust conversion of protein sequence alignments into the corresponding codon alignments. *Nucleic Acids Res.* **34**, W609–W612 (2006).
47. Birney, E., Thompson, J. D. & Gibson, T. J. PairWise and SearchWise: finding the optimal alignment in a simultaneous comparison of a protein profile against all DNA translation frames. *Nucleic Acids Res.* **24**, 2730–2739 (1996).
48. Nei, M. & Gojobori, T. Simple methods for estimating the numbers of synonymous and nonsynonymous nucleotide substitutions. *Mol. Biol. Evol.* **3**, 418–426 (1986).
49. Virtanen, P. et al. SciPy 1.0: fundamental algorithms for scientific computing in Python. *Nat. Methods* **17**, 261–272 (2020).
50. Michael Delaine-Smith, R., Javaheri, B., Helen Edwards, J., Vazquez, M. & Rumney, R. M. H. Preclinical models for in vitro mechanical loading of bone-derived cells. *Bonekey Rep.* **4**, 728 (2015).

Acknowledgements

This study was supported by the Sigrid Juselius Foundation, JSPS Grants-in-Aid for Scientific Research (JP23K08670), the Murata Foundation and the Turku Collegium for Science, Medicine and Technology. This study was supported by the IT-CSC Finland (Project ID #2004931). We thank Erasmus+ undergraduate students Ms. Valentine Jarry and Ms. Aude I Sanchez for their help in performing the mechanical loading experiments and other members and collaborators of the Phylobone project for helpful discussions. We thank Ms. Samira El Manfi from Prof. Ulvi Gursoy's group, Ms. Katja Sampalahti, Ms. Tatjana Peskova, and Dr. Vuokko Loimaranta for their technical assistance in performing the Western blotting. We also thank the two anonymous reviewers for their constructive and thorough reports.

Author contributions

M.N. and P.P. conceived and designed the study. S.S., K.H., M.F-R., and M.N. performed cell experiments. C.B., M.F-R. and P.P. performed bioinformatics analyses. M.N. and P.P. analyzed the data and had full access to the experimental data in the study, and took responsibility for the integrity and accuracy of the data analysis. M.N. and P.P. carried out data acquisition and prepared the manuscript. All authors approved the final version of the manuscript.

Competing interests

The authors declare no competing interests.

Additional information

Supplementary information The online version contains supplementary material available at <https://doi.org/10.1038/s42003-025-09292-1>.

Correspondence and requests for materials should be addressed to Pere Puigbò or Miho Nakamura.

Peer review information *Communications Biology* thanks Raquel Ruivo and the other, anonymous, reviewer(s) for their contribution to the peer review of this work. Primary Handling Editors: Michele Repetto and George Inglis.

Reprints and permissions information is available at <http://www.nature.com/reprints>

Publisher's note Springer Nature remains neutral with regard to jurisdictional claims in published maps and institutional affiliations.

Open Access This article is licensed under a Creative Commons Attribution-NonCommercial-NoDerivatives 4.0 International License, which permits any non-commercial use, sharing, distribution and reproduction in any medium or format, as long as you give appropriate credit to the original author(s) and the source, provide a link to the Creative Commons licence, and indicate if you modified the licensed material. You do not have permission under this licence to share adapted material derived from this article or parts of it. The images or other third party material in this article are included in the article's Creative Commons licence, unless indicated otherwise in a credit line to the material. If material is not included in the article's Creative Commons licence and your intended use is not permitted by statutory regulation or exceeds the permitted use, you will need to obtain permission directly from the copyright holder. To view a copy of this licence, visit <http://creativecommons.org/licenses/by-nc-nd/4.0/>.

© The Author(s) 2025